tube-generated flow possesses the characteristics of isotropic turbulence far enough downstream of the tube array as in the case of concentric porous tube array.[1] The results are shown in Fig. 4, with $c$ being the tube spacing. The turbulent energy in both cases is roughly the same at eight tube spacings from the tube grid (i.e., $x/c \approx 9$). The eccentric tube data show that the turbulent energy decays thereafter as $(x/c)^{-2}$, which is different from the $(x/c)^{-1.1}$ dependence observed by Avidor,[1] Gas-El-Hak,[3] and Tassa.[4] Based on Taylor's hypothesis of frozen convection, the scale size was computed from the measured average velocity and autocorrelations using the relation $L_f = u\int_0^\infty R(\tau)\,d\tau$. The eccentric porous tube data show a substantially smaller scale size which increase approximately as $(x/c)^{0.9}$, slightly different from the linear increase observed in the concentric tube-generated flow.

### Acknowledgment

This work was supported by Naval Research under Contract No. N00014-76-C-0040.

### References

[1] Avidor, J. M., Kemp, N. H., and Knight, C. J., "Experimental and Theoretical Investigation of Flow Generated by an Array of Porous Tubes," *AIAA Journal*, Vol. 14, Nov. 1976, pp. 1534-1540.

[2] Tong, K.-O, Knight, C. J., and Avidor, J. M., "Flow Generated by an Array of Eccentric Porous Tubes," AIAA Paper 77-662, Albuquerque, N. Mex., 1977.

[3] Gad-El-Hak, M. and Corrsin, S., "Measurements of Nearly Isotropic Turbulence Behind a Uniform Jet Grid," *Journal of Fluid Mechanics*, Vol. 62, Jan. 1974, pp. 115-143.

[4] Tassa, Y. and Kamotani, Y., "Experiments on Turbulence Behind a Grid with Jet Injection in Downstream and Upstream Direction," *The Physics of Fluids*, Vol. 18, April 1975, pp. 411-414.

# Numerical Method for Boundary Layers with Blowing—The Exponential Box Scheme

T. M. El-Mistikawy* and M. J. Werle†
*University of Cincinnati, Cincinnati, Ohio*

## Introduction

NUMERICAL solutions of boundary-layer flows in the presence of massive injection through a porous surface are complicated by the multistructure nature of the flowfield. This Note presents a new numerical scheme based on exponential difference operator concepts,[1-5] combined with Keller's box scheme approach[6] to produce a stable second-order accurate finite-difference scheme for such convection-diffusion problems. The technique developed here is demonstrated through application to the self-similar boundary-layer equations with massive blowing at the surface.

## Governing Equations and Solution Method

Attention here is directed toward solution of the Falkner-Skan equations with blowing given here as

Received Nov. 22, 1977; revision received March 21, 1978.

Index categories: Boundary Layers and Convective Heat Transfer—Laminar; Computational Methods.
*Graduate Research Assistant, Dept. of Aerospace Engineering and Applied Mechanics.
†Professor, Dept. of Aerospace Engineering and Applied Mechanics; currently Chief, Gas Dynamics Section, United Technologies Research Center, East Hartford, Conn. Member AIAA.

$$V_\eta + F = 0, \quad F_{\eta\eta} - VF_\eta + \beta(1-F^2) = 0 \tag{1}$$

with

$$F(0) = 0, \quad V(0) = V_w, \quad F \to 1 \text{ as } \eta \to \infty \tag{2}$$

where $V_w$ is related to the physical injection velocity, $F$ represents the normalized longitudinal velocity component, and $\beta$ the inviscid pressure-gradient parameter.

In the present study, an iterative numerical approach is used to first write the momentum equation as

$$F_{\eta\eta} - (a+b)F_\eta + abF = -\beta \tag{3}$$

where $a$ and $b$ are assumed to be known from a previous iteration and are given as

$$a \equiv V/2 + \sqrt{(V/2)^2 + \beta F}, \quad b \equiv V/2 - \sqrt{(V/2)^2 + \beta F} \tag{4}$$

A departure is now made from the classical approach of solving Eq. (3) using Taylor's series to generate difference approximations to derivatives over a small grid distance. Following the lead of Refs. 1-5, the coefficients of Eq. (3) are first approximated over each small grid distance by constants, and the resulting equation integrated exactly. The resulting solution between points 1 and 2 of Fig. 1 is:

$$F_{1,2} = A_1 e^{a_1\eta} + B_1 e^{b_1\eta} + f_1 \tag{5}$$

where $f_1 \equiv -\beta/a_1 b_1$, and the coefficients $a_1$, $b_1$ are evaluated at the midpoint of the grid indicated. Use of Eq. (5), a similar expression for $F_{2,3}$ in the interval between points 2 and 3, and the two continuity conditions that $F_{2+} = F_{2-}$ and $F_{\eta 2+} = F_{\eta 2-}$ produce the difference relation

$$r_1 F_1 - (s_1 + s_2)F_2 + r_2 F_3 = (r_1 - s_1)f_1 + (r_2 - s_2)f_2 \tag{6}$$

where

$$r_1 = (a_1 - b_1)e^{b_1 \Delta\eta_1}/t_1, \quad r_2 = (a_2 - b_2)e^{-a_2 \Delta\eta_2}/t_2 \tag{7a}$$

$$s_1 = [a_1 - (1-t_1)b_1]/t_1, \quad s_2 = [a_2(1-t_2) - b_2]/t_2 \tag{7b}$$

$$t_1 = 1 - e^{-(a_1 - b_1)\Delta\eta_1}, \quad t_2 = 1 - e^{-(a_2 - b_2)\Delta\eta_2} \tag{7c}$$

Equation (6) is a three-point difference approximation to Eq. (3) that produces an easily solvable tridiagonal set of algebraic equations. In addition, it possesses all the favorable properties of both the exponential and "two-point" or "box" scheme approaches (Ref. 6). It is found to be diagonally dominant for $ab < 0$, it is second-order accurate in $\Delta\eta_i$ throughout the diffusion region, and most important, it automatically and smoothly switches to a second-order accurate windward difference scheme as the normal convection velocity $V$ (as represented by the term $a+b$) becomes large, negative or positive.

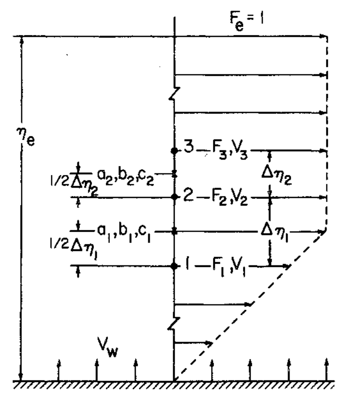


**Fig. 1 Nomenclature and grid geometry.**

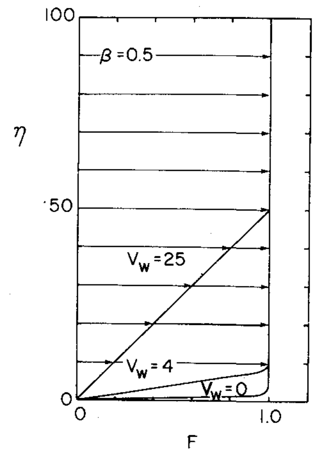


**Fig. 2 Longitudinal velocity profiles.**

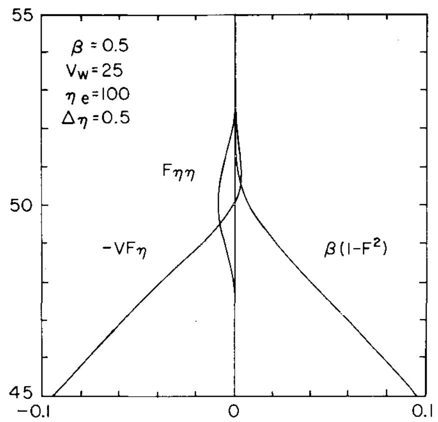


**Fig. 3 Momentum balance components.**

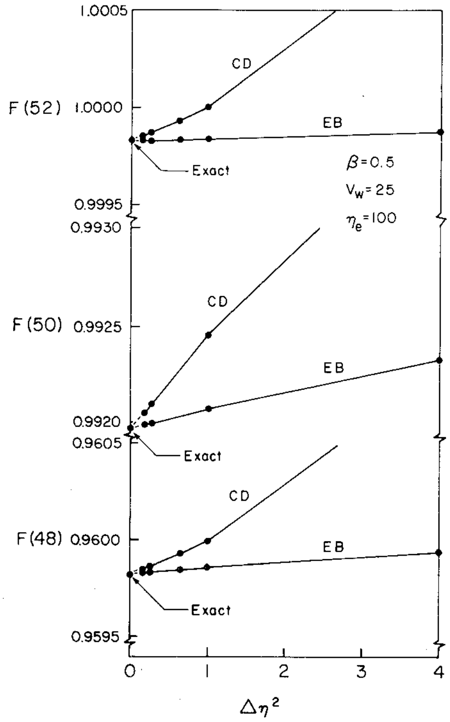


**Fig. 4 Error assessment.**

The companion difference representation of the continuity equation given in Eq. (1) is obtained by direct substitution of Eq. (5) and integrating analytically over each cell of the mesh.

## Results and Discussion

The present exponential box (EB) scheme has been applied and verified for a wide range of test cases,[7] with only typical results presented here. Longitudinal velocity profiles are shown in Fig. 2 for blowing at an axisymmetric stagnation point ($\beta = 0.5$), where the massive blowing case ($V_w = 25$) is similar to the cold-wall case presented by Liu and Chiu.[8] The present case, however, was for an adiabatic wall condition and was chosen to allow isolated study of the EB scheme for the momentum and continuity equations alone.

Figure 3 shows the multistructure nature of the flow by giving the individual component contributions to the governing momentum balance equation in the critical region of the flow ($45 \leq \eta \leq 55$). Clearly, the flow represents an inviscid process below $\eta = 48$, where the normal convection and pressure gradient effects totally balance one another. Only above this region does the diffusion effect play a significant role. With so much of the flow basically inviscid in nature, it should not be surprising to find that diffusion-type numerical schemes, such as the classical three-point central difference scheme, have difficulty representing this flow. Such difficulties usually manifest themselves in terms of nonmonotonic (jagged) velocity distributions (or local "wiggles"). This point is discussed further in Ref. 7 with the conclusion that this difficulty is largely due to a failure of central difference schemes to adequately model the normal convection effects. It is verified in Ref. 7 that a "windward" representation of the convection terms is needed to represent such flows properly. The exponential box scheme developed here automatically and smoothly switches from a second-order accurate diffusion-type scheme in diffusion regions ($\eta > 48$) to a second-rder accurate windward scheme in normal convection-dominated regions ($\eta < 48$), thus encountering no numerical difficulties or "instabilities" even for a constant grid mesh as per Ref. 8. The accuracy and reliability of the current approach is attested to in Fig. 4, where the results of a typical step size study is shown for three points in the critical region of the flowfield, $45 \leq \eta \leq 55$. Here the EB scheme is seen to maintain second-order accuracy (i.e., produce a straight-line variation with $\Delta\eta^2$) for a uniform step size $\Delta\eta$ as large as two, while a central difference scheme (CD) rapidly loses its second-order nature. Reference 7 presents a more detailed comparison and shows the current approach to be superior to four other difference methods as well.


## Acknowledgment

This work was partially supported by the NASA Langley Research Center under Grant NSG 1208 and the Air Force Flight Dynamics Laboratory Contract No. F33615-76-C-3091.


## References


[1] Allen, D. N. de G. and Southwell, R. V., "Relaxation Methods Applied to Determine the Motion in Two Dimensions of a Viscous Fluid Past a Fixed Cylinder," *Quarterly Journal of Mechanics and Applied Mathematics*, Vol. 8, 1955, pp. 129-145.

[2] Dennis, S. C. R., "Finite Differences Associated with Second-Order Differential Equations," *Quarterly Journal of Mechanics and Applied Mathematics*, Vol. 23, 1960, pp. 487-507; see also, "The Numerical Solution of the Vorticity Transport Equation," appearing in *Lecture Notes in Physics*, Vol. 19, Springer-Verlag, 1973, pp. 120-129.

[3] Pruess, S. A., "Solving Linear Boundary Value Problems by Approximating the Coefficients," *Mathematics of Computation*, Vol. 27, 1973, pp. 551-561.

[4] Rosé, M. E., "Weak-Element Approximations to Elliptic Differential Equations," *Numerische Mathematik*, Vol. 24, 1975, pp. 185-204.

[5] Roscoe, D. F., "New Methods for the Derivation of Stable Difference Representations for Differential Equations," *Journal of the Institute of Mathematics and Its Applications*, Vol. 16, 1975, pp. 291-301.

[6] Keller, H. B., *Numerical Methods for Two-Point Boundary Value Problems*, Blaisdel Publishing Co., 1968.

[7] El-Mistikawy, T. M. and Werle, M. J., "Numerical Methods for Inviscid/Viscous Fluid Flows," University of Cincinnati, Dept. of Aerospace Engineering Rept. No. AFL 77-9-34, Sept. 1977.

[8] Liu, T. M. and Chiu, H. H., "Fast and Stable Numerical Method for Boundary Layer Flow with Massive Blowing," *AIAA Journal*, Vol. 14, Jan. 1976, pp. 114-116.

# Aerodynamics of Slender Lifting Surface in Accelerated Flight

Shigenori Ando*
*Nagoya University, Nagoya, Aichi, Japan*

## I. Introduction

THERE are many researches into the aerodynamics of lifting surfaces in unsteady motion. Most of these, however, concern out-of-plane motions at a uniform flight speed, with few studies for nonuniform flight speeds.[1,2,3] These problems have become increasingly more important, because recent airplanes, such as STOL or supersonic, can experience considerable acceleration during the take-off climb or landing approach. More precise estimation of take-off or landing distance would require some aerodynamic theories for accelerated flight.

In Ref. 4, a fundamental formulation was made for wings in nonuniform motion in an inviscid incompressible flow. A Fourier transform for the in-plane coordinate variables was used. In Ref. 5, application was made to two-dimensional airfoils with a sinusoidally pulsating speed. A significant result was the fact that the difference between unsteady and quasi-steady lifts is significant, as was also shown by the previous writers.[2,3] In general, the lift of a wing depends on the complete history of its motion, and not just on the instantaneous acceleration.

In this paper, we treat the problem of slender wings in accelerated motion. This problem also is solvable and represents the low aspect ratio limit of wing theory opposite that of the two-dimensional problem. An interesting result has been obtained in that the lift force for slender wings is shown to depend only on the instantaneous acceleration and not on the history of its motion. An acceleration (deceleration) increases (decreases) the lift from that for the uniform flight speed.

## II. General Formulation

In this section, a general formulation is given for the case of a wing in nonuniform motion (flight speed) in an inviscid fluid. The analysis employs a moving axes system fixed to the wing. According to Reissner,[6] the unsteady linear equations of aerodynamics expressed in a moving axes system can be written as follows:

$$u_i' = \nabla\phi \tag{1}$$

$$p_i/\rho = (U+\Omega\times r)\cdot\nabla\phi - \partial\phi/\partial t \tag{2}$$

$$\nabla^2\phi - (1/a_0^2)[\partial/\partial t - (U+\Omega\times r)\cdot\nabla]^2\phi = 0 \tag{3}$$

$$(\partial\phi/\partial n)\,|\nabla F_{Lp}| = (U+\Omega\times r)\cdot\nabla f_L - \partial f_L/\partial t \tag{4}$$

Here $u_i'$ denotes the velocity of a fluid particle relative to the inertia system (fixed to the earth), the subscript $i$ denotes disturbances, $\phi$ is the velocity potential, $r=ix+jy+kz$ denotes the position of a fluid particle relative to the moving axes system, $p$ and $\rho$ denote pressure and mass density of the air, respectively, $U$ and $\Omega$ denote the linear and angular velocities of the moving axes system relative to the inertia system, respectively, $a_0$ is the sonic speed in the undisturbed condition, and $t$ is time. An equation for the wing surfaces may be written as

$$F_L(x,y,z,t) = F_{Lp} - f_L = 0 \tag{5}$$

where $F_{Lp}$ concerns the fundamental wing surface making no disturbances, $f_L$ concerns a small out-of-plane displacement, $\nabla$ stands for $i\partial/\partial x + j\partial/\partial y + k\partial/\partial z$. Equations (1-4) are valid for subsonic, transonic, and supersonic regions, provided that the fluid is inviscid and the disturbances are small.

We also make the following three additional assumptions:

1) The wing makes only a straight translation in still air in the negative-$x$ direction

$$U = -U(t)i \qquad u_0' = 0 \quad \Omega = 0 \tag{6}$$

2) The wing lies nearly in the $xy$ plane

$$F_{Lp} - f_L = z - f_L(x,y,t) = 0 \tag{7}$$

3) The flight velocity $U(t)$ is nonzero and positive. Then we may replace time, $t$ with the flight distance $\tau$, defined as follows:

$$\tau = \int_0^t U(t_1)\,\mathrm{d}t_1 \tag{8}$$

Thus,

$$\partial/\partial t + U(t)\,\partial/\partial x = \tilde{U}(\tau)\,(\partial/\partial x + \partial/\partial\tau) \qquad U(t)\equiv\tilde{U}(\tau) \tag{9}$$

and Eqs. (1-4) reduce to

$$u_i' = \nabla\phi \tag{10}$$

$$p_i/\rho = -\tilde{U}(\tau)\,(\partial/\partial x + \partial/\partial\tau)\phi \tag{11}$$

$$\nabla^2\phi = (1/a_0^2)[\tilde{U}(t)\,(\partial/\partial x + \partial/\partial\tau)]^2\phi \tag{12}$$

$$\partial\phi/\partial z = +\tilde{U}(\tau)\,(\partial/\partial x + \partial/\partial\tau)f_L \tag{13}$$

The governing differential equation, Eq. (12), may be rewritten in a more explicit form:

$$[1-\tilde{M}_0^2(\tau)]\phi_{xx} + \phi_{yy} + \phi_{zz} = \tilde{M}_0^2(\tau)[2\phi_{x\tau} + \phi_{\tau\tau} + (\tilde{U}'/\tilde{U})\,(\phi_x + \phi_\tau)] \tag{14}$$

where $M_0(t)\equiv\tilde{M}_0(\tau)$ denotes instantaneous flight Mach number and $\tilde{U}'(\tau) = \mathrm{d}\tilde{U}/\mathrm{d}\tau$.

Although Eq. (14) is linear in the velocity potential $\phi$, it contains variable coefficients dependent on $\tau$. Hence, we cannot use the concept of frequency response, and analytically solvable cases may be rare. Two simple cases exist, one for two-dimensional airfoils, the other for slender wings. The latter is discussed in the following sections.

## III. Slender Wing in Accelerated Flight

Let us denote $l_x$, $l_y$, and $l_z$ as the reference lengths in the $x,y,z$ directions, assuming $l_y = l_z \equiv l$. We also denote $t_1$ and $\tau_1$ as the reference time and flight distance, and assume $\tau_1 = Ut_1$. In the special case when the flight speed is simply harmonic in time with period $T_1$, we may take $t_1 = T_1$. Using the con-

Received Dec. 1, 1977; revision received Feb. 9, 1978. 

Index categories: Aerodynamics; Performance.

*Professor, Department of Aeronautical Engineering. Member AIAA.